A Novel Pattern Diversity Reflector Antenna Using Reconfigurable Frequency Selective Reflectors

I-Young Tarn and Shyh-Jong Chung, *Senior Member, IEEE*

***Abstract*—A radiation pattern diversity reflector antenna is investigated. Novel switchable frequency selective reflectors are designed and developed to construct a square corner reflector antenna. By controlling a switching device on the frequency selective reflector, one can make it opaque or transparent to a vertically polarized incident wave. This antenna is fed by a monopole. By configuring the switch states of the frequency selective reflectors, various beam shapes can be formed and steered. Measured results of the antenna show good agreement with the calculated ones.**

***Index Terms*—Corner reflector, radiation pattern diversity, reconfigurable frequency selective reflector.**

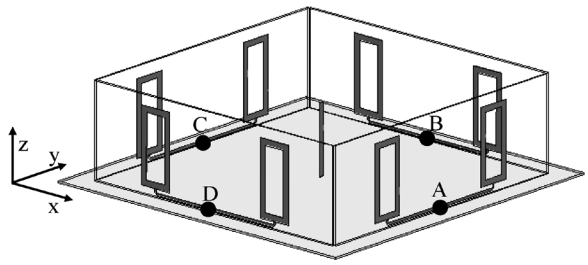

Fig. 1. Configuration of the pattern reconfigurable reflector antenna.

I. Introduction

FOR utilizing the limited spectrum efficiently, the technology of radiation pattern reconfigurable antennas [1]–[15] is often applied. The radiation pattern diversity operation offers optimized coverage by producing stronger gains in specific directions to increase the power intensity of the signal and an omni-directional pattern when communication in all directions is required. This type of antennas is an excellent candidate to reduce the multi-path interference and to enhance the communication link performance because of the adaptive patterns it provides.

Many pattern reconfigurable antennas stem from Yagi-Uda antenna design [4]–[10] and switched parasitic array [11]–[15]. The directivity and orientation of the radiation pattern are under the control of different combinations of switching states. This provides a simple and flexible way for pattern beam-forming. In [4], an active monopole is surrounded by a relatively large number of parasitic elements terminated by two different switchable loads. Whereas in [5]–[7], the antennas maintain the basic Yagi-Uda type but the parasitic monopole elements around the active monopole antennas are loaded alternatively, either short or open. Since the loads attached to the parasitic monopoles alter the effective lengths of monopoles, the electromagnetic interactions between monopoles result in beam-formed patterns. Cylindrical rod monopoles are used in [5] and [7], while cylindrical rod monopoles with disc plates which help reducing the height of antenna are disclosed in [6]. In [8]–[10], printed strips on the substrate are adopted for use as the active and parasitic monopoles instead of the cylindrical rod monopoles to reduce the complexity substantially. The switched printed parasitic monopoles are length-tunable by directly changing the length of short-ended parasitic monopoles with switches [10]–[12].

In this paper, a new pattern reconfigurable antenna, which has the same applications and similar results as [11] and [12] yet based on a thoroughly different principle, is proposed. This antenna, which evolved from the corner reflector antenna, has four rectangular plates standing erectly on the ground plane and enclosing the substrate backed strip monopole in the center. Each rectangular plate is a reconfigurable frequency selective reflector (RFSR) with two loop resonant elements, whose transmission/reflection characteristic is designed to be controlled by one switching device. That is, only four switches are enough for configuring the reflection states of the four side walls of the proposed 90° corner reflector antenna, so as to adaptively form the radiation patterns. The switching circuitry, bias lines, and impedance matching networks of this antenna are hidden beneath the ground plane, which can avoid the undesired electromagnetic interactions. In addition, this antenna features beam tilting property, which can reduce the co-channel interference. Thus, it is highly suitable for modern base station antenna applications and the areas of WiFi and WLAN networks.

The proposed antenna innovatively combines an inventive RFSR design concept and the idea of realizing the pattern diversity function by corner reflector antenna. Moreover, these two individual methodologies developed can be extended for future reconfigurable electromagnetic structure designs and radiation pattern reconfigurable antennas respectively, so they are worth paying more attention to and making further investigations.

II. Antenna Configuration

The pattern reconfigurable reflector antenna, as shown in Fig. 1, comprises a feeding monopole antenna in the center, four rectangular plates on the sidewalls of the square corner reflector antenna, and a finite square ground plane on which the former

Manuscript received June 11, 2008; revised December 31, 2008. First published July 28, 2009; current version published October 07, 2009. This work was supported in part by the National Science Council under Contract NSC 96-2752-E-009-003-PAE.

I.-Y. Tarn is with the Electrical Engineering Division, National Space Organization, Hsinchu 310, Taiwan (e-mail: ian.tarn@gmail.com).

S.-J. Chung is with the Department of Communication Engineering, National Chiao Tung University, Hsinchu 310, Taiwan (e-mail: sjchung@cm.nctu.edu.tw).

Digital Object Identifier 10.1109/TAP.2009.2028606

elements are mounted. Planar RFSR is applied to implement the rectangular plates on the sidewalls. The transmission and reflection property of the RFSR can be controlled by changing the switch state. For one state the RFSR acts as a metal plate, while for the other state it is transparent to the waves from/to the feed antenna. Four switches (A, B, C and D) connecting the frequency selective elements on the RFSR and the ground plane are located on the four sides respectively. The pattern of a corner reflector antenna varies with the number and the arrangement of the reflectors. With various combinations of the switch states, multiple patterns can thus be formed.

The ground plane, which is also the reference for the impedance matching circuit, was made on the top surface of an FR4 substrate with dielectric constant of 4.4. The matching microstrip line for the center feed antenna was printed on the backside of the same substrate, and prior to that, the impedance of the fabricated antenna had been measured. In the proposed antenna configuration, the switches and their associated circuitry, e.g., the bias lines, can be placed behind the ground plane but not within the region where electromagnetic waves propagate. This arrangement minimizes the adverse influence caused by the undesired yet necessary presence of those elements.

The center frequency of the pattern diversity reflector antenna is designed at 2.45 GHz. A quarter-wavelength monopole serves as the driving element, which is a 29.8 mm $\times$ 2.4 mm metal strip printed on a 1.6-mm thick, 4-mm wide and 30.5-mm long FR4 substrate.

A conventional corner reflector is a directional antenna consists of two intersecting flat conducting plates of infinite extent. The pattern shape, gain and feed point impedance are all functions of the feed-to-corner spacing and corner angle [16]–[18]. Finite extent plates will result in a pattern broader than that for infinite plates. In addition, the height of the plate is usually chosen to be from 1.2 to 1.5 times the length of the feed so as to minimize the direct radiation by the monopole feed into the back region. The heights of the reflectors are thus designed to be 40 mm in this work.

In order to obtain multiple symmetric patterns, RFSRs with identical dimensions are used to construct the reflector plates in this work. Initially, the vertical reflector surfaces and the horizontal ground plane were assumed to be perfectly conductive. The vertical feed monopole was in the center of the reflectors. Corner reflector antennas with the reflector surfaces forming an equilateral triangle, a square, a pentagon, a hexagon and an octagon in various sizes were analyzed. Among these, the square one was selected because it has the best directivity with any two adjacent reflector surfaces being perfect conductors and the other two surfaces being void. Fig. 2 shows the simulated peak gains for various widths of the two adjacent reflectors. The maximum peak gain is 7.30 dBi when the widths are 120 mm. The reflector plates were then determined to be 120 mm $\times$ 40 mm and the ground plane measures 140 mm $\times$ 140 mm. The simulated 3-D pattern of a corner reflector antenna in this configuration is displayed in Fig. 3. The peak gain is at ($\theta = 42^\circ$, $\phi = 225^\circ$), the 3-dB beamwidth is about 105° and the 3-dB beamwidth in the XY plane is about 60°. Enlarging the heights of the reflector plates will improve the directivity but at the cost of the increased antenna volume.

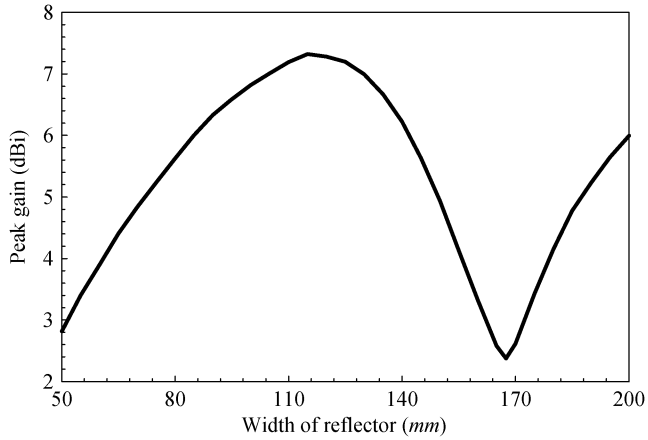

Fig. 2. Simulated peak gains of the square corner reflector for various widths of the reflectors with the heights of the reflector fixed at 40 mm.

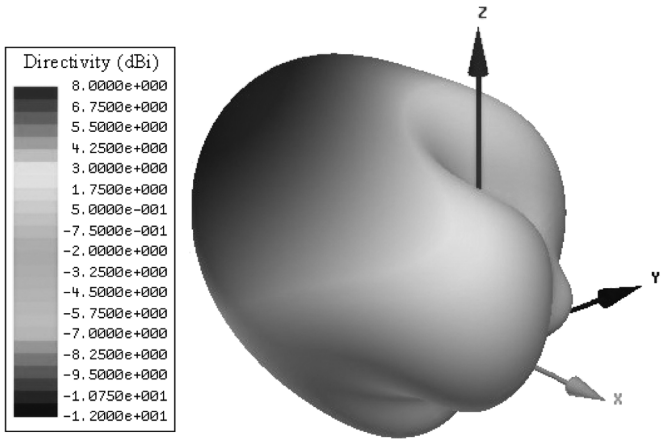

Fig. 3. Simulated 3-D pattern of the square corner reflector antenna.

III. Novel Reconfiguralbe Frequency Selective Reflector

The notion of the RFSR originates from the frequency selective surface. A frequency selective surface is usually an assembly of identical elements periodically arranged in a one or two dimensional array that can provide frequency filtering to incoming electromagnetic waves. Similar to the frequency filters in traditional RF circuits, the frequency selective surface may have bandpass or band-stop spectral behavior. The frequency response of the reflection (or transmission) coefficient for a frequency selective surface depends on the geometry of its constituent elements and the arrangement of the array. The frequency response is changeable. In general, a great number of actuators [19], PIN diodes, MEMS switches, or silicon switches [20]–[23] are needed. In this paper, a simple design with minimized number of switches is proposed to develop the RFSR.

Researches on both the underlying theories and practices of many frequency selective elements have been well established [24]–[26]. Square loop element is the one having simple and effective structure. It has a relatively wide frequency bandwidth, and its resonant frequency is fairly stable with respect to changes in incident angle and polarization. Besides, the reflection phase curves of the square loop structures are less sensitive to oblique incidence [27]–[29].

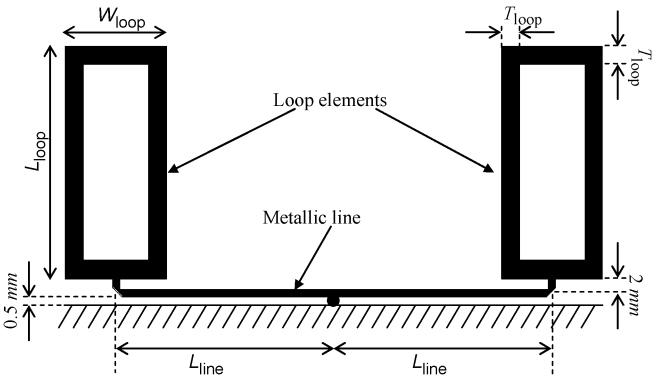

Fig. 4. Geometry and parameters of the RFSR.

In virtue of its symmetric geometry, the square loop elements works well for circular polarization waves. Nonetheless, the feed monopole in this paper is a linear polarization antenna. That means the width and length of the loop have not to be the same; there are more degrees of freedom in design to fit the frequency selective structures into the reflector plates of the corner reflector antenna at the same time maintain good performance. Therefore, this type of element, more exactly the rectangular loop, was adopted for this work.

In principle, the total length of a loop type resonator should be about one wavelength. As shown in Fig. 4, two parallel rectangular loop elements are printed on a 120 mm $\times$ 40 mm FR4 substrate with thickness of 0.8 mm. A printed metallic line with a length of about a half wavelength is created to connect these two rectangular loops. The frequency selective elements are designed such that whose current distributions change significantly with the switching state and hence there would be a conspicuously difference in frequency response.

Consider first the case where only two rectangular loops exist on each reflector plate but without the connecting metallic line. When a vertically (z-) polarized plane wave is incident normally on the rectangular loops, strong currents with distributions like Fig. 5(a) would be induced due to the resonance of the loops. The induced currents on the two vertical segments of each loop have the maximum levels and keep in the same direction. Notably, due to symmetry, the center points of horizontal segments of the loops are open-circuited and thus have vanishing currents. The strong in-phase currents on the vertical segments of the loops re-radiate the electromagnetic field toward both sides of the reflector plate. The re-radiated field would cancel the incident field in the wave incoming direction while generate a wave propagating toward the opposite direction. That is, the incident waves are reflected.

Now consider the existence of the metallic line connecting the loops. This line, together with the horizontal ground plane, forms a half-wavelength transmission line. As a normally incident plane wave illuminates on the rectangular loops, all the induced currents should be symmetrical to the perpendicular plane passing the midpoint of the metallic line. It means that the current at the midpoint is null and the transmission line shows an open circuit at that position. This open circuit then causes short circuits at the two ends of the line when transformed back through the quarter-wavelength transmission line segments, which in turn destroys the resonant current distributions on the loops. The induced currents on these out-of-resonance loops would become weak, as shown in Fig. 5(b), and thus produce negligible re-radiation fields. The reflector plate is thus transparent to the incident wave. It is noticed that although horizontal currents are induced on the metallic line, the contributed re-radiation fields can be ignored due to the cancellation from the image currents (not shown in the figure) on the ground plane.

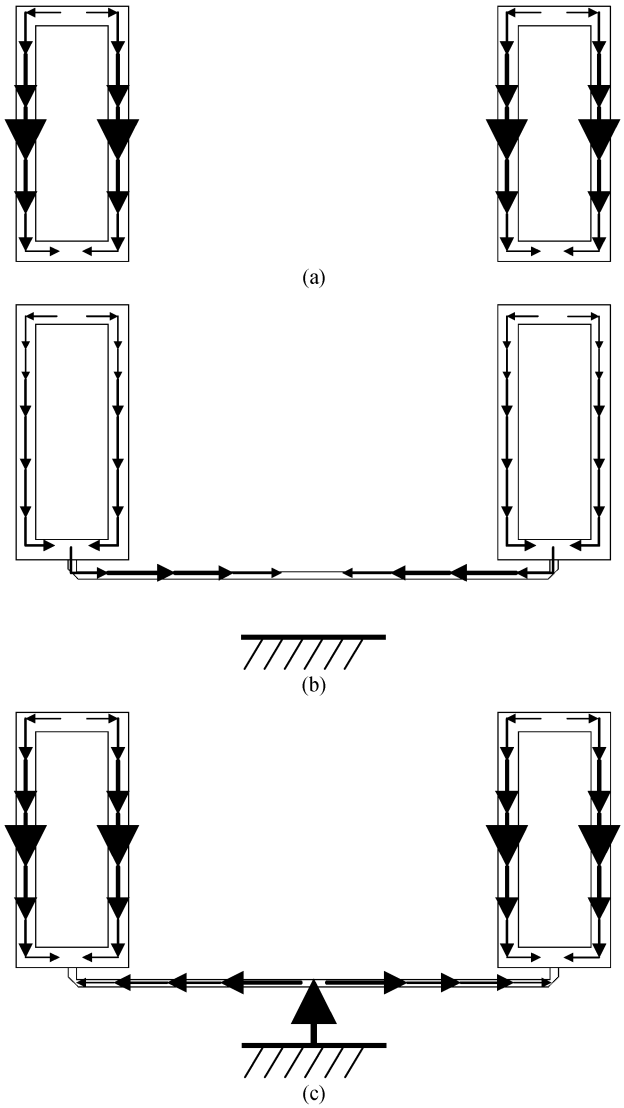

Fig. 5. (a) Induced currents on the two rectangular loop elements. (b) Induced currents on the proposed RFSR in the off-state. (c) Currents caused by terminating the middle of the metallic line to the ground.

On the other hand, when the midpoint of the metallic line is short-circuited to the ground by a switch, the half-wavelength transmission line appears open-circuited at the two ends and thus supplies no current to the loops. The rectangular loops would therefore retain the strong resonant currents as shown in Fig. 5(c). Under this condition, the reflector plate will reflect back the incident wave as in the case without the metallic line.

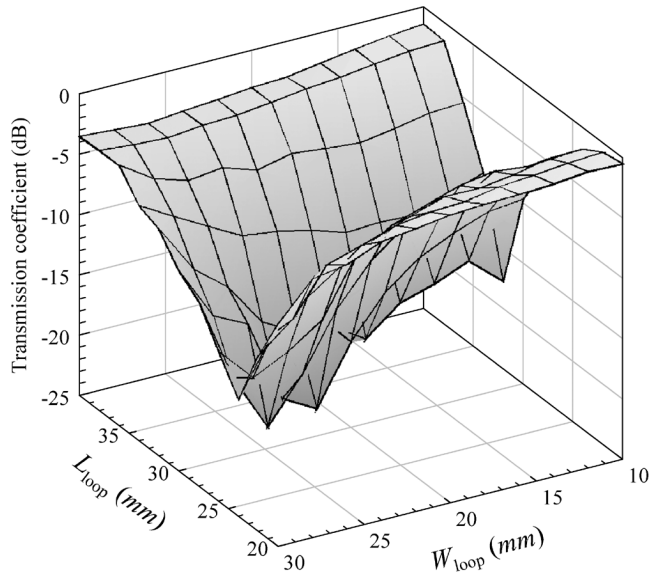

Fig. 6. Simulated on-state transmission coefficients for various $L_{\rm loop}$ and $W_{\rm loop}$ at 2.45 GHz.

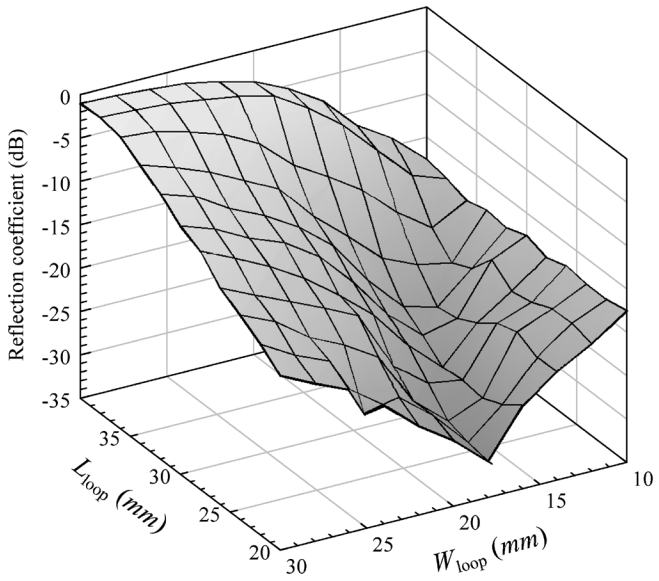

Fig. 7. Simulated off-state reflection coefficients for various $L_{\rm loop}$ and $W_{\rm loop}$ at 2.45 GHz.

The full-wave electromagnetic software Ansoft HFSS [30] was employed to analyze the RFSR structure. The rectangular loop element on the RFSR is designed to resonate at 2.45 GHz for vertically polarized plane waves. The simulated on-state transmission and off-state reflection coefficients for a normally incident plane wave are plotted in Fig. 6 and Fig. 7 respectively. The loop sizes $L_{\rm loop}$ and $W_{\rm loop}$ are varied with constant metal width $T_{\rm loop}(=\ 2.5$ mm) and metallic line's length $2L_{\rm line}(=60$ mm). Here, a short metal strip connecting the midpoint of the metallic line and the ground plane is used to imitate the switch in on-state, and nothing between the midpoint and the ground represents the switch in off-state. As observed from the figures, when $L_{\rm loop}=32$ mm and $W_{\rm loop}=14$ mm, a low transmission coefficient for the on-state and a low reflection coefficient for the off-state are obtained.

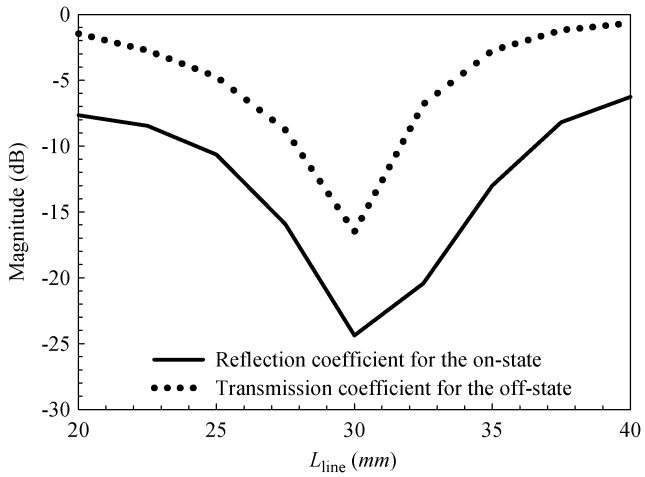

Fig. 8. Simulated on-state transmission coefficients and off-state reflection coefficients at 2.45 GHz for various Lline ($L_{\rm loop}=32$ mm, $W_{\rm loop}=14$ mm, and $T_{\rm loop}=2.5$ mm).

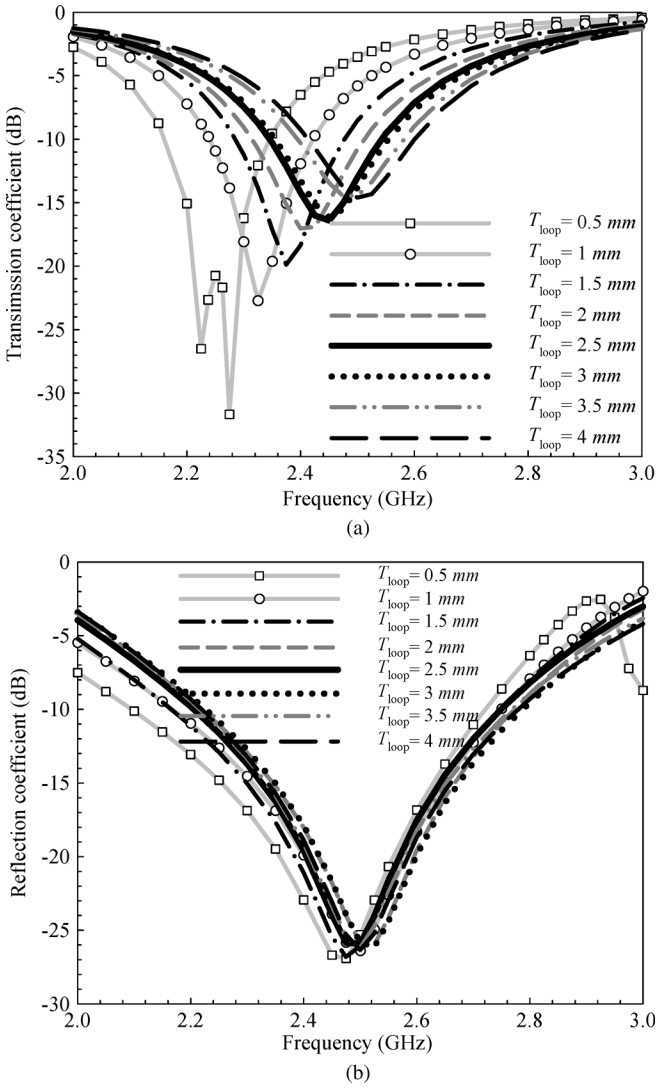

Fig. 9. (a) Transmission coefficient curves for various widths of the loop in the on-state. (b) Reflection coefficient curves for various widths of the loop in the off-state.

Then, the frequency selective property with respect to the transmission line was analyzed. It is found from Fig. 8 that the

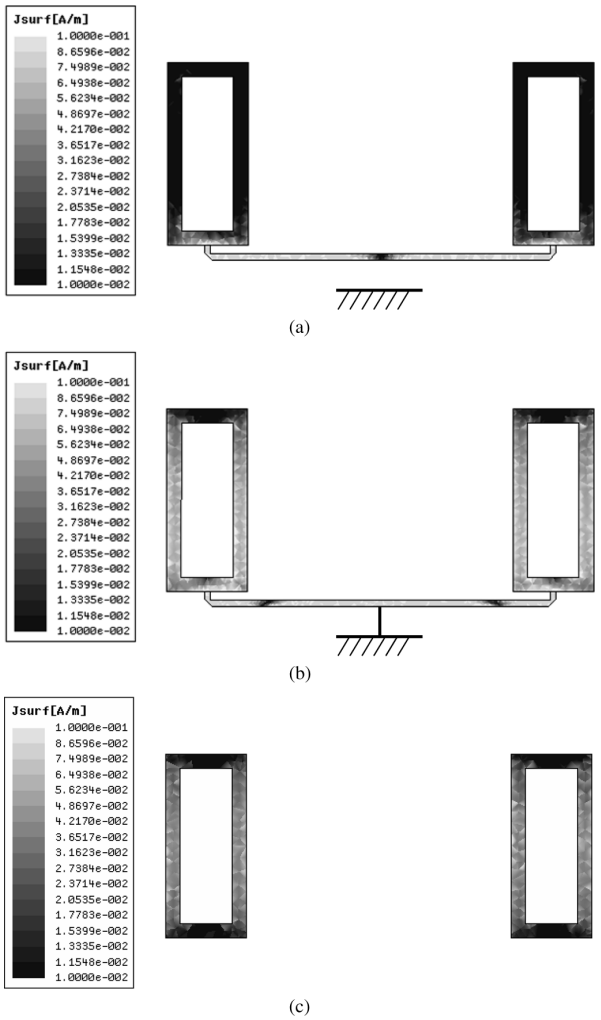

Fig. 10. (a) Simulated induced current density distribution for the proposed design in the off-state. (b) Simulated induced current density distribution for the proposed design in the on-state. (c) The simulated induced current density distribution over the rectangular loops.

length of the printed metallic line should be 60 mm ($L_{\text{line}} = 30$ mm). The width of the line yields no significant effect on the electrical length and was set to 1 mm. The spacing between metallic line and the ground plane is 0.5 mm.

However, the trace width of the loop (T_{loop}) is an important parameter. A greater T_{loop} results in a wider transmission bandwidth and tends to resonate at higher frequency for the on-state, while the reflection curves scarcely vary with T_{loop} for the off-state, as shown in Fig. 9. T_{loop} is determined to be 2.5 mm such that this design is opaque ($\text{transmission coefficient} = -16.4$ dB) in the on-state and transparent ($\text{reflection coefficient} = -23.9$ dB) in the off-state at 2.45 GHz.

The simulated induced current density distributions for 2.45 GHz vertically polarized waves for the proposed design in the off-state and on-state are shown in Fig. 10(a) and Fig. 10(b) respectively. The current density distribution over the rectangular loops only, without the metallic line, is also depicted in Fig. 10(c) for comparison. Due to the proximity coupling between the rectangular loops and the metallic line near the joining points, the two opens in the on-state (Fig. 10(b)) do not exactly occur at the joining points but move closer towards the center. However, the geometrical resonances still remain. It is obvious that the induced currents on the rectangular loops in Fig. 10(b) and Fig. 10(c) are approximately the same level and much stronger than that in the off-state (Fig. 10(a)).

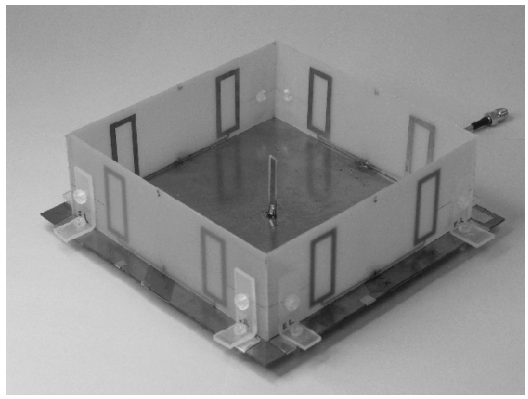

Fig. 11. Photo of the finished pattern reconfigurable reflector antenna.

TABLE I
DEFINITIONS OF THE SIX FUNDAMENTAL CASES AND THEIR CORRESPONDING PARAMETERS OF THE PATTERN RECONFIGURABLE REFLECTOR ANTENNA

		Case 1	Case 2	Case 3	Case 4	Case 5	Case 6
Switch states	A	1	0	1	0	0	1
	B	1	0	1	1	1	1
	C	0	0	1	0	0	0
	D	0	0	1	0	1	1
Simulated peak gain direction		θ= 39°, ϕ= 225°	Omni	Omni	θ= 39°, ϕ= 270°	θ= 39°, ϕ= 0° & ϕ= 180°	θ= 36°, ϕ= 180°
Simulated 3-dB beamwidth		147°	N/A	N/A	190°	N/A	159°
Simulated peak gain (dBi)		6.77	2.71	3.26	5.24	4.66	6.19

IV. MEASUREMENT RESULTS

The photograph of the finished antenna is shown in Fig. 11. Radiation patterns with different shapes and orientations can be achieved by various combinations of the switch states. The on- and off-states were realized by directly soldering the middle point of the metallic line to the ground plane and de-soldering respectively.

Due to the symmetry of the antenna architecture, there are six fundamental cases. The definitions of the cases and their corresponding antenna parameters are listed in Table I, where 0 stands for switch off and 1 for switch on. The 3-dB beamwidths are the half-power beam angles in the azimuth plane with θ at the peak gain directions. It is clear that Case 1, 4 and 6 have directional patterns while Case 1 produces the maximum gain. The pattern of Case 5 is bidirectional because two of the switches on the opposite sides are in the same state and vice versa. When the switches are all on or all off, the pattern is omni-directional.

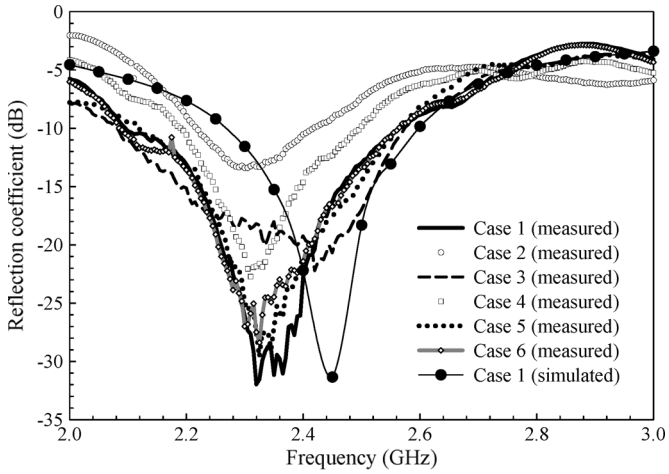

Fig. 12. Reflection coefficients of the finished antenna.

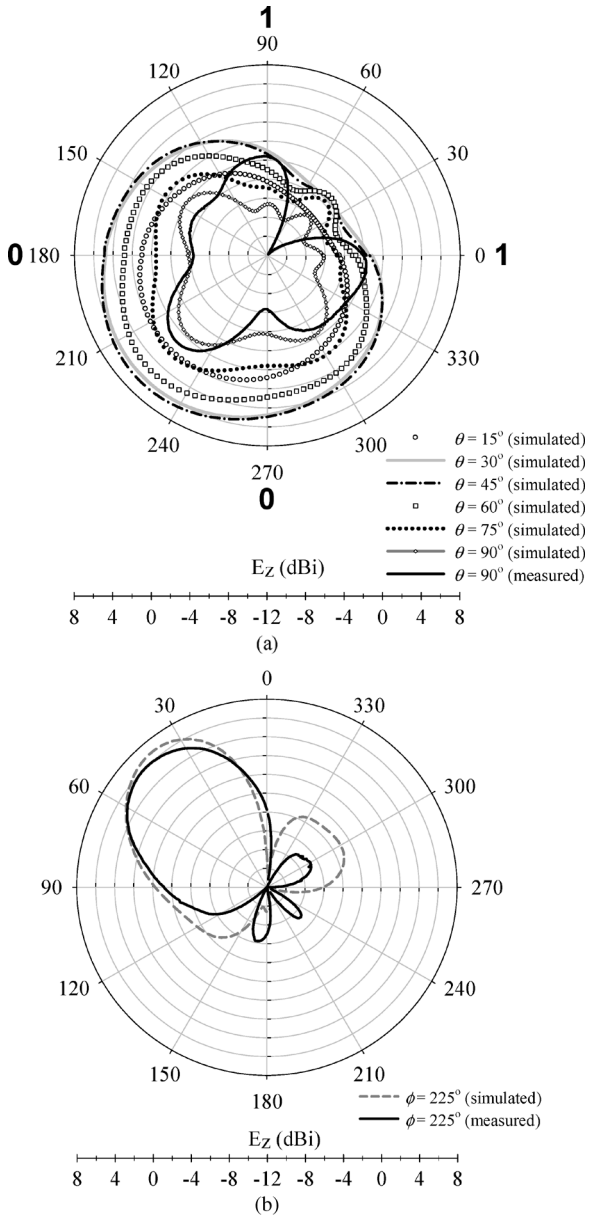

Fig. 13. Simulated and measured patterns of Case 1 at 2.45 GHz (a) for various azimuth cuts, and (b) in $\phi = 225^\circ$ plane.

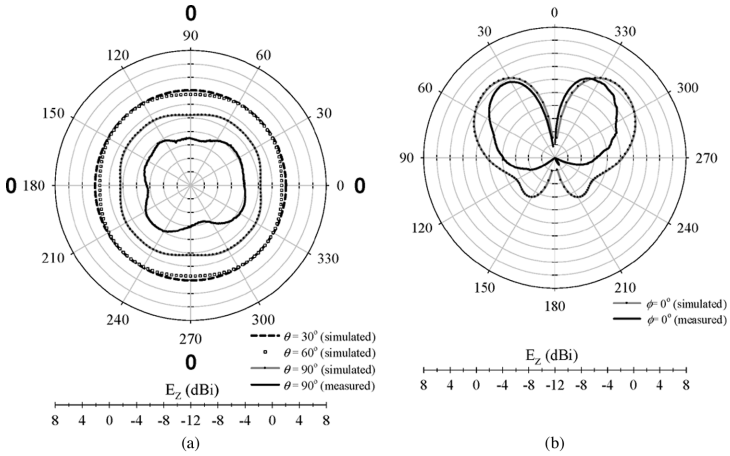

Fig. 14. Simulated and measured patterns of Case 2 at 2.45 GHz (a) for various azimuth cuts, and (b) in $\phi = 0^\circ$ plane.

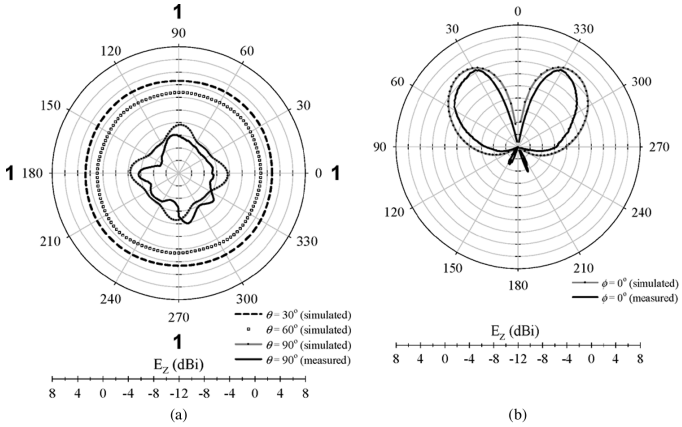

Fig. 15. Simulated and measured patterns of Case 3 at 2.45 GHz (a) for various azimuth cuts, and (b) in $\phi = 0^\circ$ plane.

Since Case 1 provides the maximum peak gain, the impedance of the active element was matched under this case. The measured reflection coefficients of the finished antenna for the six cases against frequency, and the simulated result of Case 1, are shown in Fig. 12. It can be seen that the −10 dB bandwidth for Case 1 is from 2.09 GHz to 2.57 GHz (about 19.6%). The narrowest bandwidth occurs for Case 2, which is only 200 MHz (from 2.22 GHz to 2.42 GHz). The bandwidths of the other cases cover at least 2.19–2.50 GHz.

The measured co-polarization patterns of Case 1, a directional case with the highest gain, at the 2.45 GHz are displayed in Fig. 13. As can be seen, the measured patterns agree well with the simulated ones in the main beam region, whereas with dissimilar side-lobes. The peak gain of 5.99 dBi was measured at ($\theta = 45^\circ$, $\phi = 225^\circ$). The measured side-lobe level and 3-dB beamwidth in $\phi = 225^\circ$ plane are 12.17 dB and 52°, respectively. The measured patterns of Case 2 to Case 6 are shown in Fig. 14 to Fig. 18. Their peak gains are 1.74, 2.47, 3.05, 3.61, and 5.60 dBi, respectively. Case 2 is the one whose measured pattern less closely coincides with the simulated one, while the other cases exhibit good consistency. Obviously, the patterns are apt to be directional with their main lobes pointed toward the orientation where the switch states are off. It is evident from

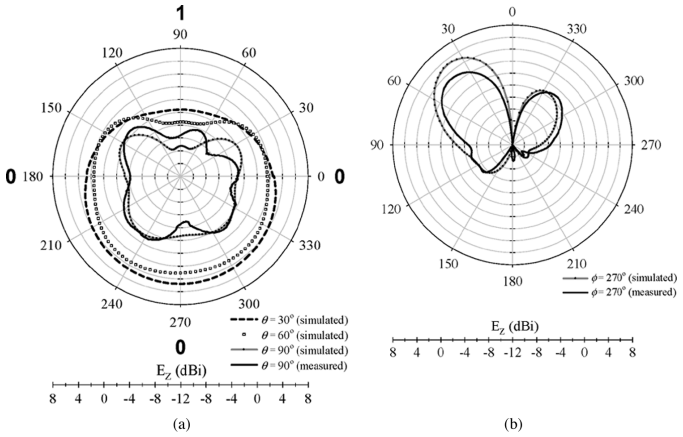

Fig. 16. Simulated and measured patterns of Case 4 at 2.45 GHz (a) for various azimuth cuts, and (b) in $\phi = 270^\circ$ plane.

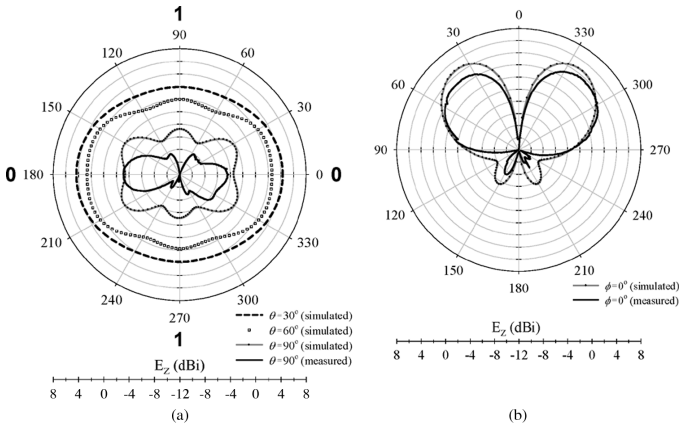

Fig. 17. Simulated and measured patterns of Case 5 at 2.45 GHz (a) for various azimuth cuts, and (b) in $\phi = 0^\circ$ plane.

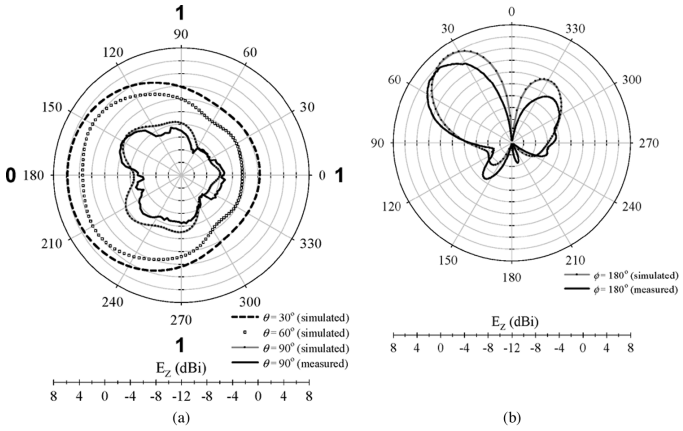

Fig. 18. Simulated and measured patterns of Case 6 at 2.45 GHz (a) for various azimuth cuts, and (b) in $\phi = 180^\circ$ plane.

these results that multiple shapes of patterns, both omni and directional, are provided with this antenna.

The simulated antenna radiation efficiencies of all cases are around 98%. The power dissipation mainly takes place in the substrate because of the high loss tangent of FR4. In practice, except for Case 4 and Case 5, the measured efficiencies are higher than 80%. The reason why those two cases are less efficient could be the imperfection in workmanship of the RFSR plates on A and C sides, which causes a little higher reflection in off-state than that of the others two plates.

V. Conclusion

In this paper, a radiation pattern reconfigurable antenna has been presented. It evolved from the corner reflector antenna. A novel concept has been proposed to control a surface to be transmissive or reflective to waves at designated frequency with only one switching device. The RFSR plates were used on the side walls of the corner reflector antenna. This antenna provides six fundamental patterns by various combinations of the switch states. The pattern can also be steered to rotate in azimuth plane electronically. By comparison, the maximum measured peak gain of the finished antenna is 5.99 dBi, and the maximum simulated peak gain of 6.77 dBi is close to the maximum achievable gain of 7.30 dBi that assumes the side walls of the corner reflector antenna to be perfect conductors instead of RFSRs in the same configuration. This fact shows the RFSR plates in this antenna are nearly perfectly conductive when acting as reflectors and almost transparent when in the other state. A better gain and improved back-lobes could be accomplished by increasing the dimensions of the reflectors.

The successful development of the antenna demonstrates the feasibility and performances of using the concept of corner reflector to realize the radiation pattern diversity. It is possible to extend this type of antenna to circular polarization version and for multi-band operation on the basis of investigations in this work.

References

[1] A. Mehta and D. M. Syahkal, "Spiral antenna with adaptive radiation pattern under electronic control," in *Proc. IEEE Int. Symp. Antennas Propag.*, Jun. 2004, vol. 1, pp. 843–846.

[2] A. Mehta, H. Nakano, and D. M. Syahkal, "A switched beam single arm rectangular spiral antenna with hybrid switch network," in *Proc. IEEE Int. Symp. Antennas Propag.*, Jul. 2005, vol. 2B, pp. 589–592.

[3] S. S. L. Yang and L. M. Luk, "A wideband l-probe fed patch antenna for pattern reconfigurable," in *Proc. IEEE Int. Symp. Antennas Propag.*, Jul. 2005, vol. 2B, pp. 581–584.

[4] M. D. Migliore, D. Pinchera, and F. Schettino, "A simple and robust adaptive parasitic antenna," *IEEE Trans. Antennas Propag.*, vol. 53, no. 10, pp. 3262–3272, Oct. 2005.

[5] Y. Nakane, T. Noguchi, and Y. Kuwahara, "Trial casel of equipped with switched loads on parasitic elements," *IEEE Trans. Antennas Propag.*, vol. 53, no. 10, pp. 3398–3402, Oct. 2005.

[6] M. R. Kamarudin and P. S. Hall, "Disc-loaded monopole antenna array for switched beam control," *Electron. Lett.*, vol. 42, no. 2, pp. 66–67, Jan. 2006.

[7] R. Vaughan, "Switched parasitic elements for antenna diversity," *IEEE Trans. Antennas Propag.*, vol. 47, no. 2, pp. 399–405, Feb. 1999.

[8] H. S. M. Elkamchouchi and H. E.-D. M. Hafez, "Switchable beam diversity antenna," in *Proc. 3rd Int. Conf. Microw. Millimeter Wave Technol.*, Aug. 17–19, 2002, pp. 377–380.

[9] C. Laohapensaeng, C. Free, and K. M. Lum, "Printed strip monopole antenna with the parasitic elements on the circular ground plane," in *Proc. IEEE Int. Workshop in Antenna Technology: Small Antennas and Novel Metamaterials*, Mar. 7–9, 2005, pp. 371–374.

[10] S. Zhang, G. H. Huff, J. Feng, and J. T. Bernhard, "A pattern reconfigurable microstrip parasitic array," *IEEE Trans. Antennas Propag.*, vol. 52, no. 10, pp. 2773–2776, Oct. 2004.

[11] M. L. Lee, Y. S. Wang, and S. J. Chung, "Pattern reconfigurable strip monopole with eight switched printed parasitic elements," in *Proc. IEEE Int. Symp. Antennas Propag.*, Jun. 2007, pp. 3177–3180.

[12] J. C. Ke, C. W. Ling, and S. J. Chung, "Implementation of a multi-beam switched parasitic antenna for wireless applications," in *Proc. IEEE Int. Symp. Antennas Propag.*, Jun. 2007, pp. 3368–3371.

[13] L. Petit, L. Dussopt, and J.-M. Laheurte, "MEMS-switched parasitic-antenna array for radiation pattern diversity," *IEEE Trans. Antennas Propag.*, vol. 54, no. 9, pp. 2624–2631, Sep. 2006.
[14] J. Sun, W. Chen, and Z. Feng, "A novel dielectric-supported switched parasitic antenna array," in *Proc. IEEE Int. Symp. Antennas Propag.*, Jul. 9–14, 2006, pp. 2325–2328.
[15] S. C. Panagiotou, T. D. Dimousios, S. A. Mitilineos, and C. N. Capsalis, "Broadband switched parasitic arrays for portable DVB-T receiver applications in the VHF/UHF bands," *IEEE Antennas Propag. Mag.*, vol. 50, no. 5, pp. 110–117, Oct. 2008.
[16] W. L. Stutzman and G. A. Thiele, *Antenna Theory and Design*. New York: Wiley, 1997.
[17] N. Inagaki, "Three-dimensional corner reflector antenna," *IEEE Trans. Antennas Propag.*, vol. 22, no. 4, pp. 580–582, Jul. 1974.
[18] N. Inagaki, K. Uchikawa, Y. Hashimoto, and N. Kukuma, "3-D corner reflector antenna and its analysis using UTD," in *Proc. IEEE Int. Symp. Antennas Propag.*, Jun. 20–24, 1994, vol. 1, pp. 598–601.
[19] D. Lockyer, C. Moore, R. Seager, R. Simpkin, and J. C. Vardaxoglou, "Coupled dipole arrays as reconfigurable frequency selective surfaces," *Electron. Lett.*, vol. 30, no. 16, pp. 1258–1259, Aug. 4, 1994.
[20] J. P. Gianvittorio, J. Zendejas, Y. Rahmat-Samii, and J. W. Judy, "Reconfigurable MEMS-enabled frequency selective surfaces," *Electronics Lett.*, vol. 38, no. 25, pp. 1627–1628, Dec. 5, 2002.
[21] J. P. Gianvittorio, J. Zendejas, Y. Rahmat-Samii, and J. W. Judy, "MEMS enabled reconfigurable frequency selective surfaces: Design, simulation, fabrication, and measurement," in *Proc. IEEE Int. Symp. Antennas Propag.*, Jun. 16–21, 2002, vol. 2, pp. 404–407.
[22] X. Liang, L. Li, J. A. Bossard, and D. H. Werner, "Reconfigurable frequency selective surfaces with silicon switches," in *Proc. IEEE Int. Symp. Antennas Propag.*, Jul. 9–14, 2006, pp. 189–192.
[23] J. A. Bossard, D. H. Werner, T. S. Mayer, and R. P. Drupp, "Reconfigurable infrared frequency selective surfaces," in *Proc. IEEE Int. Symp. Antennas Propag.*, Jun. 20–25, 2004, vol. 2, pp. 1911–1914.
[24] B. A. Munk, *Frequency Selective Surfaces: Theory and Design*. New York: Wiley, 2000.
[25] G. H.-H. Sung, K. W. Sowerby, and A. G. Williamson, "Equivalent circuit modelling of a frequency selective plasterboard wall," in *Proc. IEEE Int. Symp. Antennas Propag.*, Jul. 2005, vol. 4A, pp. 400–403.
[26] D.-G. Youn, K.-H. Kim, Y.-C. Rhee, S.-T. Kim, and C.-C. Shin, "Experimental development of 2.45 GHz rectenna using FSS and dual-polarization," in *Proc. 30th Eur. Microw. Conf.*, Oct. 2000, pp. 1–4.
[27] A. Pirhadi, M. Hakkak, F. Keshmiri, and R. K. Baee, "Design of compact dual band high directive electromagnetic bandgap (EBG) resonator antenna using artificial magnetic conductor," *IEEE Trans. Antennas Propag.*, vol. 55, no. 6, pp. 1682–1690, Jun. 2007.
[28] T. K. Wu, "Double-square-loop FSS for multiplexing four (S/X/Ku/Ka) bands," in *Proc. IEEE Int. Symp. Antennas Propag.*, Jun. 24–28, 1991, vol. 3, pp. 1885–1888.
[29] Y.-Y. Gu, W.-X. Zhang, Z.-C. Ge, and Z.-G. Liu, "Research on reflection phase characterizations of artificial magnetic conductors," in *Proc. Asia-Pacific Microwave Conf.*, Dec. 4–7, 2005, vol. 3.
[30] HFSS Ansoft Corporation. Pittsburgh, PA.

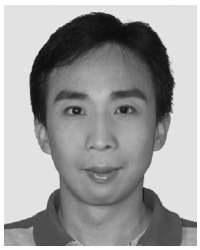

I-Young Tarn was born in Taipei, Taiwan. He received the B.S. and M.S. degrees in electrical engineering from Yuan-Ze University, Tao-Yuan, Taiwan, in 1993 and 1995, respectively, and is currently working toward the Ph.D. degree in communication engineering at the National Chiao Tung University, Hsinchu, Taiwan.

From 1995 to 1999, he was an Assistant Researcher in Systems Engineering Project, National Space Program Office, Hsinchu, Taiwan, R.O.C. Since 2000, he has been with the Electrical Engineering Division of the National Space Organization, where he has been involved in satellite communications and antenna design. His research interests include microwave/mm-wave planar antennas, reflectarray antennas, circular polarization selective structures and satellite antenna design and verification.

Shyh-Jong Chung (M'92–SM'06) was born in Taipei, Taiwan. He received the B.S.E.E. and Ph.D. degrees from National Taiwan University, Taipei, Taiwan, in 1984 and 1988, respectively.

Since 1988, he has been with the Department of Communication Engineering, National Chiao Tung University, Hsinchu, Taiwan, where he is currently a Professor. From September 1995 to August 1996, he was a Visiting Scholar with the Department of Electrical Engineering, Texas, A&M University, College Station. He has authored or coauthored over 70 technical papers in international journals or conferences including several invited papers and speeches. His areas of interest include the design and applications of active and passive planar antennas, communications in intelligent transportation systems (ITSs), LTCC-based RF components and modules, packaging effects of microwave circuits, and numerical techniques in electromagnetics.

Dr. Chung serves as the Chairman of IEEE MTT-S Taipei Chapter from 2005. He was also the Treasurer of IEEE Taipei Section from 2001 to 2003.